

# c-Abl antagonizes the YAP oncogenic function

R Keshet<sup>1</sup>, J Adler<sup>1</sup>, I Ricardo Lax<sup>1</sup>, M Shanzer<sup>1</sup>, Z Porat<sup>2</sup>, N Reuven<sup>1</sup> and Y Shaul<sup>\*,1</sup>

YES-associated protein (YAP) is a central transcription coactivator that functions as an oncogene in a number of experimental systems. However, under DNA damage, YAP activates pro-apoptotic genes in conjunction with p73. This program switching is mediated by c-Abl (Abelson murine leukemia viral oncogene) via phosphorylation of YAP at the Y357 residue (pY357). YAP as an oncogene coactivates the TEAD (transcriptional enhancer activator domain) family transcription factors. Here we asked whether c-Abl regulates the YAP–TEAD functional module. We found that DNA damage, through c-Abl activation, specifically depressed YAP–TEAD-induced transcription. Remarkably, c-Abl counteracts YAP-induced transformation by interfering with the YAP–TEAD transcriptional program. c-Abl induced TEAD1 phosphorylation, but the YAP–TEAD complex remained unaffected. In contrast, TEAD coactivation was compromised by phosphomimetic YAP Y357E mutation but not Y357F, as demonstrated at the level of reporter genes and endogenous TEAD target genes. Furthermore, YAP Y357E also severely compromised the role of YAP in cell transformation, migration, anchorage-independent growth, and epithelial-to-mesenchymal transition (EMT) in human mammary MCF10A cells. These results suggest that YAP pY357 lost TEAD transcription activation function. Our results demonstrate that YAP pY357 inactivates YAP oncogenic function and establish a role for YAP Y357 phosphorylation in cell-fate decision.

*Cell Death and Differentiation* (2015) 22, 935–945; doi:10.1038/cdd.2014.182; published online 31 October 2014

The Hippo pathway is an evolutionarily conserved pathway initially identified in the fly as a controller of organ size.<sup>1–3</sup> In mammals, recent studies have established a role for this pathway in regulating cell contact inhibition, organ size control, and cancer development.<sup>4–6</sup> The Hippo pathway is activated upon sensing of cell–cell contact via cell surface molecules. These upstream elements transmit the signal through effectors that activate the kinase Mst that in turn activates the kinase Lats (large tumor suppressor), a tumor suppressor.<sup>7,8</sup> Activated Lats phosphorylates the transcriptional coactivator YES-associated protein (YAP) on five conserved HxRxxS motifs.<sup>6</sup> Phosphorylation of YAP on Serine 127 by Lats leads to its sequestration in the cytoplasm by binding to 14-3-3. Furthermore, phosphorylation of YAP by Lats primes it for degradation mediated by  $\beta$ -TrCP ( $\beta$ -transducin repeat containing E3 ubiquitin protein ligase).<sup>9</sup> Through these mechanisms the transcriptional activity of YAP is downregulated under conditions of high cell density.<sup>6,10</sup>

Although many studies on the nonreceptor tyrosine kinase c-Abl (Abelson murine leukemia viral oncogene) are focused on its role as an oncogene as part of the fusion protein BCR-Abl,<sup>11</sup> it is also known to play a role in the DNA damage response.<sup>12</sup> Once activated, c-Abl can promote apoptosis or induce cell cycle arrest through the phosphorylation and activation of p73,<sup>13,14</sup> a p53 paralog. c-Abl also phosphorylates and inhibits the E3 ligase mouse double minute 2 homolog (MDM2), resulting in stabilization of p53, the main substrate of MDM2.<sup>15</sup> Recently, c-Abl was shown to act as a

negative regulator of tumorigenic phenotype and epithelial-to-mesenchymal transition (EMT) induced by transforming growth factor- $\beta$  (TGF- $\beta$ ) in mammary cells.<sup>16</sup> Although c-Abl activation was associated with a reduction in TGF- $\beta$ -induced production of metalloproteinases that play a role in extracellular matrix remodeling by invasive tumor cells, the relevant substrates and the mechanism by which c-Abl exerts its antitumor effect on EMT and transformation in mammary cells still remains unknown.

YAP has been implicated as an oncogene in human cancers.<sup>17–19</sup> Overexpression of YAP in nontransformed human MCF10A mammary epithelial cells causes EMT, suppression of apoptosis, growth factor-independent proliferation, and anchorage-independent growth.<sup>18</sup> EMT is a normal process in development and wound healing but is also a central feature of cancer progression.<sup>20</sup> In this process, an epithelial cell loses its connection to the basement membrane and neighboring cells, loses its polarity, and acquires a fibroblast-like appearance and motility that enables it to invade tissues and propagate the tumor. Coactivation of the TEAD (transcriptional enhancer activator domain) transcription factors by YAP has been shown to be central to its promotion of proliferation and cell transformation.<sup>21</sup> Connective tissue growth factor (CTGF) and cysteine-rich angiogenic inducer 61 (Cyr61) were recently identified as YAP–TEAD target genes participating in their growth-promoting function.<sup>21,22</sup>

<sup>1</sup>Department of Molecular Genetics, Weizmann Institute of Science, Rehovot, Israel and <sup>2</sup>Biological Services Unit, Weizmann Institute of Science, Rehovot, Israel

\*Corresponding author: Y Shaul, Department of Molecular Genetics, Weizmann Institute of Science, Herzl 1, Rehovot 76100, Israel. Tel: +972 8 9342320; Fax: +972 8 9344108; E-mail: yosef.shaul@weizmann.ac.il

**Abbreviations:** c-Abl, Abelson murine leukemia viral oncogene; YAP, YES-associated protein; TEAD, transcriptional enhancer activator domain;  $\beta$ -TrCP,  $\beta$ -transducin repeat containing E3 ubiquitin protein ligase; EMT, epithelial-to-mesenchymal transition; LATS, large tumor suppressor; CTGF, connective tissue growth factor; Cyr61, cysteine-rich angiogenic inducer 61; MDM2, mouse double minute 2 homolog; TGF- $\beta$ , transforming growth factor- $\beta$ ; NES, nuclear export signal; PTPN, protein tyrosine phosphatase nonreceptor

Received 03.2.14; revised 23.9.14; accepted 26.9.14; Edited by G Melino; published online 31.10.14

Despite the demonstrated activity of YAP in the activation of pro-proliferative and anti-apoptotic genes, YAP may also exhibit proapoptotic activity under certain conditions such as DNA damage. YAP can bind to the tumor suppressor p73 through the YAP WW domain and the p73 PPPY motif.<sup>23</sup> We have previously found that like p73,<sup>13</sup> YAP is also a substrate of c-Abl and is phosphorylated at position Y357 in response to DNA damage.<sup>24</sup> YAP phosphorylated by c-Abl accumulates to higher levels, binds to p73 with higher affinity, and preferentially activates proapoptotic targets. Thus, in response to DNA damage, YAP functions as a tumor suppressor, in sharp contrast to the known oncogenic function of YAP under conditions described above.

It was recently shown that YAP can also promote colon cancer by cooperating with  $\beta$ -catenin to coactivate the transcription factor TBX5.<sup>25</sup> In this setting, YES1 tyrosine kinase phosphorylates YAP on the Y357 site. However, YES1-mediated YAP modification is oncogenic and induces assembly of the  $\beta$ -catenin–YAP complex coactivating TBX5 target genes. The fact that YAP pY357 plays two opposite roles based on the nature of the tyrosine kinase, either c-Abl or YES1, is intriguing and led us to examine YAP oncogenic potential under DNA damage and c-Abl activation. Moreover, use of a phosphomimetic YAP Y357E mutant has enabled us to analyze the effect of Yap Y357 phosphorylation independently of other effects that might be caused by active c-Abl or YES1. We report here that DNA damage specifically inhibits the YAP–TEAD transcriptional output and that the c-Abl-phosphorylated YAP is impaired in transactivation of TEAD-response genes. Remarkably, a point mutation from tyrosine to the phosphomimetic glutamate at position 357 is sufficient to cause a dramatic difference in the transforming ability of YAP. Although overexpression of wild-type YAP leads to EMT and cell transformation, the Y357E mutant is transformation incompetent. Thus, DNA damage and c-Abl determine cell fate by switching an oncogene to a tumor suppressor.

## Results

**DNA damage inhibits expression of YAP–TEAD target genes.** DNA damage activates YAP–p73 transcriptional activity through their phosphorylation by c-Abl.<sup>13,24</sup> In addition, the phosphorylation of YAP by c-Abl preferentially promotes its coactivation of pro-apoptotic genes by p73, as opposed to coactivation of Runx on non-apoptotic target genes, such as osteocalcin or Itch.<sup>26</sup> However, the question of how c-Abl-mediated YAP phosphorylation regulates TEAD coactivation remained open. To this end, we first asked whether DNA damage affects YAP–TEAD transcriptional output. Human mammary MCF10A cells were irradiated and the mRNA levels of CTGF and CYR61, two major TEAD target genes involved in cell survival, proliferation, and transformation,<sup>21,22</sup> were quantified. Interestingly, ionizing radiation (IR) inhibited the induction of these two TEAD target genes (Figure 1a). In contrast, this treatment induced the level of the endogenous pro-apoptotic PIG3 and the pro-cell cycle arrest gene p21, the well-documented p53/p73 target genes. Under DNA damage c-Abl phosphorylates YAP,<sup>24</sup> and we therefore suspected that c-Abl plays a part in mediating

this effect. Indeed, upon c-Abl depletion, CTGF expression under IR was partially restored (Figures 1b and c). Similar results were obtained with a kinase-dead c-Abl<sup>13</sup> dominant-negative mutant (Figure 1d). This effect is specific as this construct reduced the level of PIG3 and p21 induction in response to DNA damage (Figure 1e). Finally, the c-Abl inhibitor STI-571 prevented irradiation-induced reduction in CTGF transcription in a dose-dependent manner in H1299 and HepG2 cells (Figure 1f and Supplementary Figure 1). These results suggest that DNA damage, at least partially via c-Abl, reduced TEAD target genes expression.

**c-Abl inhibits YAP-induced TEAD activation.** Next we asked whether c-Abl is sufficient in inhibiting YAP-induced TEAD target genes by overexpressing active c-Abl. Under this condition, the induction of the two major TEAD target genes CTGF and Cyr61 in MCF10A cells was markedly reduced (Figure 2a) without affecting the level of YAP (Supplementary Figure 2a). In contrast, its expression in the same cells induced the level of p21 and the pro-apoptotic PUMA.

We next employed the TEAD reporter GTIIC luciferase plasmid<sup>27</sup> to investigate the c-Abl inhibitory role. Constitutively active c-Abl ( $\Delta 1-81$  c-Abl)<sup>28</sup> markedly reduced YAP coactivation of TEAD2 (Figure 2b). Unlike active c-Abl, a kinase-dead mutant of c-Abl was inefficient in inhibiting YAP–TEAD activity, indicating a kinase-dependent effect. Downregulation of YAP coactivation of endogenous TEAD by c-Abl was also demonstrated over time by real-time bioluminescence recording (Figure 2c).

Consistent with previous studies,<sup>18</sup> when overexpressed in MCF10A cells, YAP induced EMT, as evidenced by a fibroblast-like appearance and a dispersed cell distribution on a regular culture dish (Figure 2d, left panels). In contrast, MCF10A cells expressing YAP in the presence of active c-Abl displayed a cobblestone appearance similar to the control MCF10A cells. MCF10A cells form round, acini-like mammospheres when plated in 3D matrigel cultures. However, overexpression of YAP leads to large distorted mammospheres.<sup>18</sup> Overexpression of YAP in our system similarly produced large distorted structures (Figure 2d, right panels). Remarkably, cells expressing YAP together with active c-Abl resembled the phenotype of the control and formed small rounded mammospheres.

Next, we investigated the migratory potential of the different cells by using the wound healing assay. Under the assay conditions used (medium with 2% serum and no EGF) the control cells failed to migrate into the wound after 24 h, whereas YAP overexpressing cells partially filled the gap within this time period (Figure 2e). However, expression of both c-Abl and YAP dramatically reduced cell migration.

Overexpression of YAP in MCF10A induces cellular transformation, as evident from acquisition of anchorage-independent growth potential in soft agar.<sup>18</sup> Expression of c-Abl constructs robustly inhibited YAP-induced MCF10A transformation (Figure 2f and Supplementary Figure 2b) and TEAD transcriptional activity (Supplementary Figures 2c–e), consistent with its role in downregulating the YAP–TEAD transcription module. These constructs included WT c-Abl, two different constructs of constitutively active c-Abl ( $\Delta 1-81$

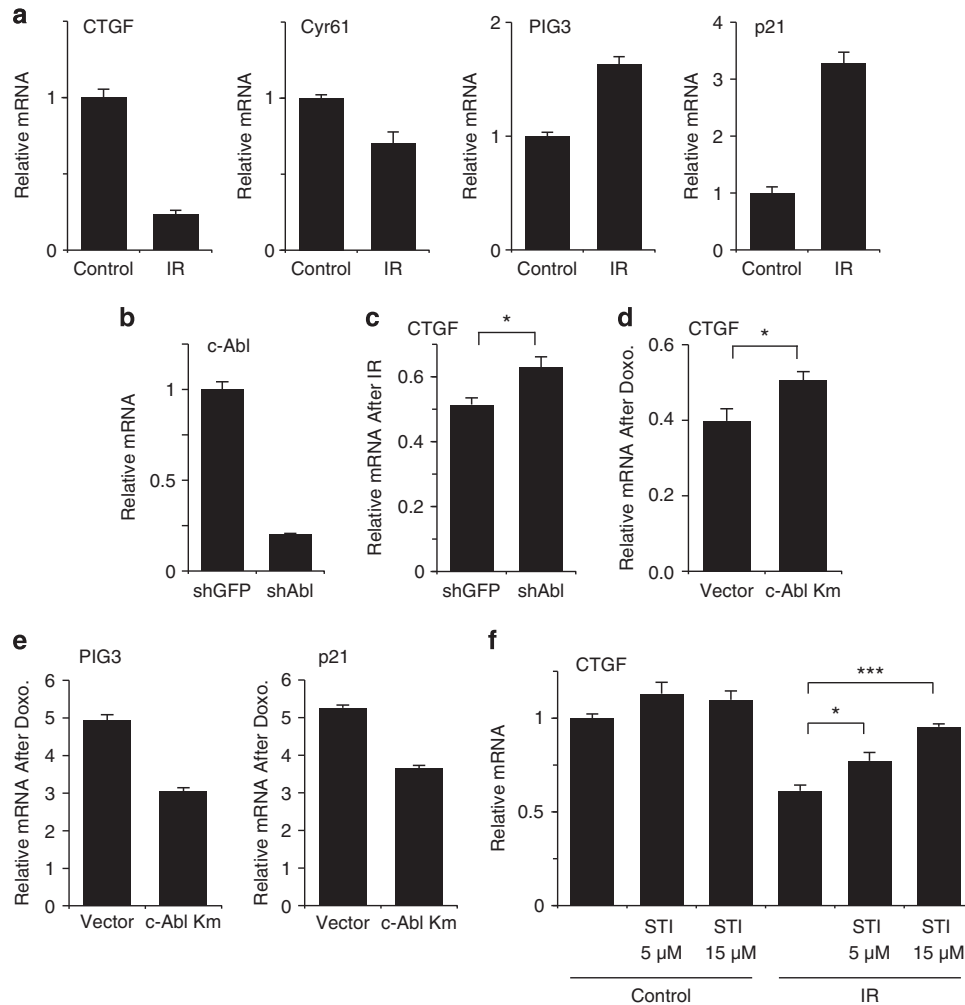


**Figure 1** DNA damage interferes with YAP and TEAD gene induction. (a) Ionizing radiation (IR) downregulates TEAD target genes. MCF10A cells were irradiated (25 Gy) and after 24 h expression of the designated genes was determined by quantitative RT-PCR and compared with nonirradiated control cells. (b) c-Abl mRNA levels in MCF10A cells infected with a lentiviral plasmid containing shRNA against either GFP or c-Abl. (c) c-Abl participates in the IR-induced downregulation of CTGF gene expression. MCF10A expressing shRNA against either GFP or c-Abl were irradiated (20 Gy) and after 24 h expression of CTGF was determined by quantitative RT-PCR ( $*P < 0.05$ ). (d and e) c-Abl participates in the doxorubicin-induced downregulation of CTGF gene expression. MCF10A expressing a kinase mutant c-Abl (c-Abl Km) or empty vector treated with 0.2  $\mu$ M doxorubicin for 24 h. Expression of genes was determined by quantitative RT-PCR ( $*P < 0.05$ ). (f) c-Abl activity is required in IR-induced inhibition of YAP–TEAD target gene expression. Human non-small-cell lung carcinoma H1299 cells were preincubated with the designated concentrations of STI-571 for 2 h and then irradiated (30 Gy). After 24 h, the expression of CTGF was analyzed as in (a). S.E. calculated from two duplicates of two independent experiments ( $*P < 0.05$ ;  $***P < 0.005$ )

c-Abl and Abl-PP),<sup>28</sup> and nuclear c-Abl, bearing no nuclear export signal (NES mutant c-Abl).<sup>29</sup> These results suggest that c-Abl inhibits YAP in coactivating TEAD, in EMT and enhanced migration induction, and in transforming MCF10A cells.

**c-Abl phosphorylates TEAD1.** The inhibitory c-Abl kinase function in YAP–TEAD activity could result from phosphorylation of either TEAD or YAP. To look for potential TEAD tyrosine phosphorylation by c-Abl, we overexpressed TEAD1 and TEAD2 with active c-Abl. Marked tyrosine phosphorylation by c-Abl was detected in TEAD1 but not in TEAD2, whereas both proteins showed an apparent accumulation in the presence of c-Abl (Figure 3a). We next compared the effect of active c-Abl on TEAD1 and TEAD2 to activate the GTIIC reporter in the presence of YAP (Figure 3b). c-Abl inhibited both to the same levels, suggesting that c-Abl

downregulation of YAP–TEAD activation does not involve phosphorylation of TEAD by c-Abl.

**The phosphomimetic Y357E mutant is inefficient in TEAD coactivation.** It is known that c-Abl phosphorylates YAP on tyrosine 357 that resides in the YAP transactivation domain<sup>24</sup> (Figure 4a). To investigate whether YAP Y357 phosphorylation by c-Abl is sufficient to blunt YAP–TEAD activation, we used YAP Y357E, a phosphomimetic YAP mutant, and YAP Y357F, a non-phosphorylatable ‘phosphodead’ mutant. The phosphomimetic strategy uncouples the direct effect of c-Abl on YAP from its other activities, such as TEAD phosphorylation. We also introduced the S127A mutation to ensure YAP nuclear localization.<sup>6</sup> MCF10A cells were stably transduced with these constructs that were expressed at the same level (Supplementary Figure 3a). Quantitative PCR analysis

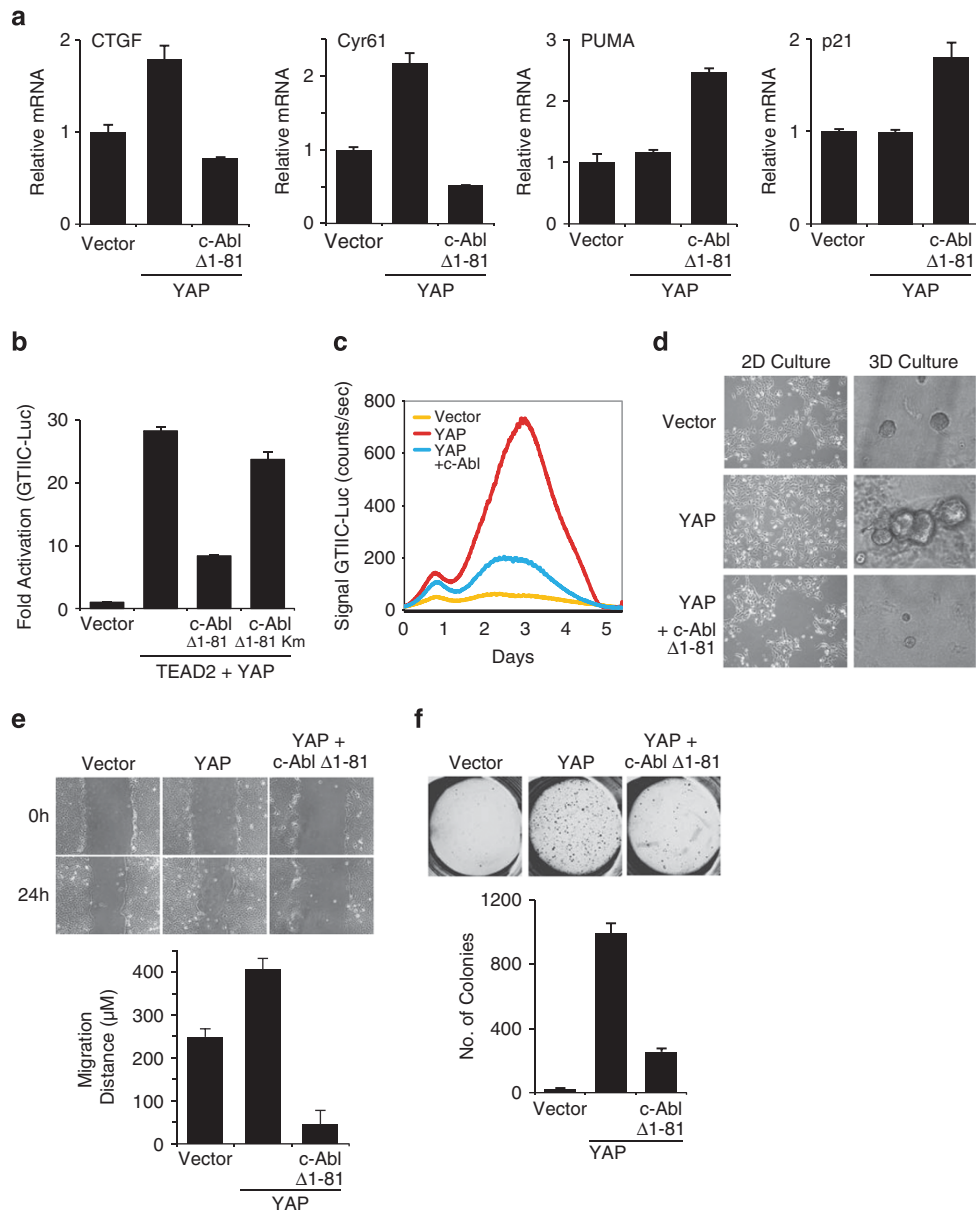


**Figure 2** c-Abl counteracts YAP-induced phenotype in MCF10A. (a) c-Abl downregulates TEAD target genes. MCF10A cells were infected with either empty vector (pBabe zeo) or YAP, and were then subjected to a second infection with either empty vector (pBabe puro) or active c-Abl. Expression of genes was determined by quantitative RT-PCR and compared with vector control cells. (b) c-Abl inhibits TEAD activation by YAP in a kinase-dependent manner. The designated plasmids were co-transfected with a TEAD-responsive element luciferase reporter plasmid (8  $\times$  GTIIC-Luc) into HEK293 cells. Luciferase activity was measured and normalized to co-transfected TK-*Renilla*. Km, kinase mutant. (c) c-Abl interferes with YAP activity over time. The designated plasmids were co-transfected with a TEAD-responsive element luciferase reporter plasmid (8  $\times$  GTIIC-Luc) into HEK293 cells and luciferase activity was recorded over 5 days using real-time bioluminescence detector. (d) c-Abl inhibits YAP-induced EMT. The 2D morphology – representative images of cells grown in monolayer cultures; 3D morphology – cells were cultured on Matrigel. Images were taken on day 4. (e) c-Abl inhibits YAP-induced enhanced migration potential as measured in a wound healing assay. Confluent cells were scratched using 1 ml pipette and grown for 24 h in medium containing 2% serum and no EGF. (f) c-Abl inhibits YAP-induced anchorage-independence. Images were taken and colonies counted 21 days after cells were seeded in soft agar. Colonies  $> 50 \mu\text{m}$  in diameter were counted as positive for growth. Upper panel: images of colonies; lower panel; quantification of colonies from three independent experiments

revealed that the phosphomimetic YAP S127A Y357E double mutant was less active in inducing endogenous CTGF and Cyr61 expression (Figures 4b and c), duplicating the c-Abl effect. Similar results were obtained when the Y357 mutations were introduced to wild-type YAP (Supplementary Figures 3b–d). This effect is specific as YAP coactivation of target genes of other transcription factors such as TBX5, p73,

and Runx was not repressed (Supplementary Figures 3e–h). The phosphomimetic YAP Y357E mutant was also less active at the level of GTIIC reporter assay (Figure 4d). Moreover, the phosphodead YAP Y357F mutant was more potent than the wild type. Expression of active c-Abl reduced the wild-type YAP transcription coactivation of TEAD to the level of that obtained with the phosphomimetic mutant. The weak effect of

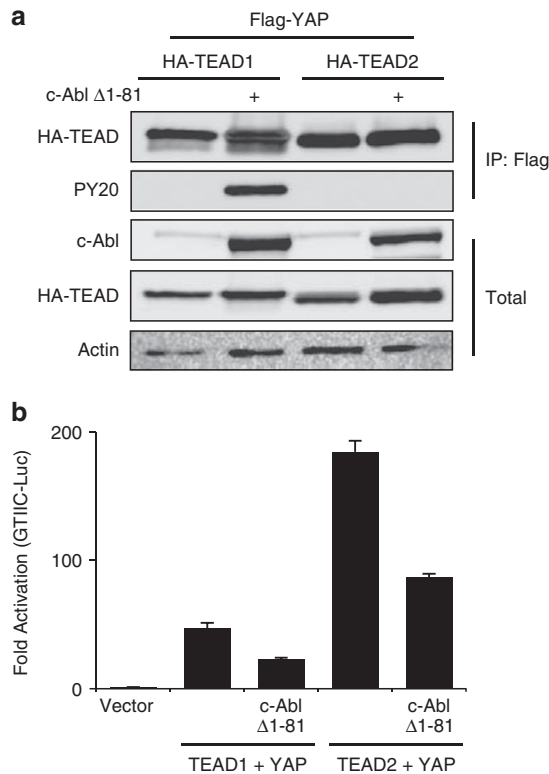


**Figure 3** c-Abl phosphorylates TEAD1. (a) c-Abl phosphorylates TEAD1 but not TEAD2. HEK293 cells were transfected with the indicated plasmids and analyzed by immunoprecipitation using HA-coated beads. Phosphorylation was detected by probing with a phosphotyrosine antibody (PY20). (b) c-Abl inhibits YAP-TEAD1 or YAP-TEAD2 to the same extent. The designated plasmids were co-transfected with a TEAD-responsive element luciferase reporter plasmid (8 × GTIIC-Luc) into HEK293 cells. Luciferase activity was measured and normalized to co-transfected TK-Renilla

the Y357E mutant is GTIIC reporter specific, and not observed with the p73 reporter (Figure 4e). These data suggest that the phosphorylation state of Y357 attenuates YAP in coactivating TEAD.

**YAP Y357 mutants are not impaired in YAP intracellular localization and TEAD binding.** The Hippo pathway controls YAP by regulating its intracellular localization. Regulation of YAP pro-proliferative function is known to be through serine phosphorylation by LATS (Figure 4a). To investigate whether the mutations at Y357 affect YAP localization, we expressed different YAP constructs fused to GFP in MCF10A cells (Supplementary Figure 4a), and YAP nuclear localization was quantified by FACS. Wild-type YAP and the Y357E and Y357F mutants were all localized mainly in the cytoplasm to the same level (Figure 5a). The YAP S127A mutant is resistant to phosphorylation by LATS and accumulates in the nucleus.<sup>6</sup> Our analysis revealed that this mutant and the double mutants S127A Y357E and S127A Y357F were all localized to the nucleus. These data suggest that Y357 mutation affects neither nuclear localization nor Lats-mediated nuclear exclusion.

YAP is known to bind TEAD through its TEAD-binding domain, an interaction critical for TEAD coactivation by YAP.<sup>21</sup> We therefore asked whether Y357E mutation affects YAP association with TEAD. HEK293 cells were co-transfected with HA-tagged TEAD1 (Figure 5b and Supplementary Figure 4b) or TEAD2 (Figure 5c) together with Flag-tagged wild-type YAP or YAP Y357E mutant constructs. No differences in the binding between TEAD isoforms and either the wild-type or the mutated YAP were observed. Similarly, active c-Abl did not reduce but rather increased the binding of YAP to TEAD1 (Supplementary Figure 4c). These results suggest that YAP Y357 phosphorylation by c-Abl does not impair YAP nuclear localization and binding to TEAD.

**The phosphomimetic Y357E mutant poorly coactivates the Gal4-TEAD chimera.** Our findings that the Y357E mutation did not affect YAP-TEAD binding or YAP localization suggested that Y357E mutation affects YAP coactivation activity. To investigate this possibility, we used a Gal4-fused TEAD construct, in which TEAD was fused to the Gal4 DNA-binding domain and the ability of Gal4-TEAD to coactivate a Gal4 luciferase reporter was measured.<sup>21</sup> By this approach we can measure direct coactivation level uncoupled from the potential effect of the YAP constructs on the TEAD DNA-binding capacity. Although the different YAP constructs were expressed at similar levels in HEK293 cells (Supplementary Figure 4d), a significant reduction in the coactivation of YAP Y357E mutant relative to wild type was obtained (Figure 5d). Interestingly, the phosphodead YAP Y357F mutant was a more potent Gal-TEAD coactivator than the wild type. Similar results were obtained using real-time bioluminescence recording (Figure 5e). These results suggest that the YAP Y357 phosphorylation state regulates TEAD coactivation, probably by modulating the recruitment of the basal transcription factors to the YAP-TEAD complex.

**YAP Y357E phosphomimetic mutant fails to induce EMT.** The lack of TEAD activation by YAP Y357E suggested that it may also be impaired in YAP-induced EMT and transformation. To test this possibility, wild-type and mutant YAP constructs were stably expressed in MCF10A cells. All three constructs were expressed at similar levels (Supplementary Figure 3b). Wild-type YAP induced EMT, as evident by the 2D culture cell morphology (Figure 6a, left panels). In contrast, MCF10A cells expressing the YAP Y357E mutant displayed a cobblestone appearance similar to the control MCF10A cells. The Y357F YAP phosphodead mutant induced a dispersed cell phenotype, suggesting that the tyrosine residue at this site is not critical for EMT. We also evaluated MCF10A mammosphere formation in a 3-dimensional culture in matrigel. Unlike wild-type YAP or phosphodead Y357F mutant overexpression, which formed large distorted structures (Figure 6a, right panels), YAP Y357E phosphomimetic mutant-expressing cells resembled the phenotype of the control and formed normal rounded mammospheres. MCF10A-YAP cells also displayed loss of cell-cell junction-localized E-cadherin, another hallmark of EMT, as shown by immunofluorescence analyses (Figure 6b). However, this phenotype was substantially diminished in YAP Y357E-expressing cells, whereas YAP

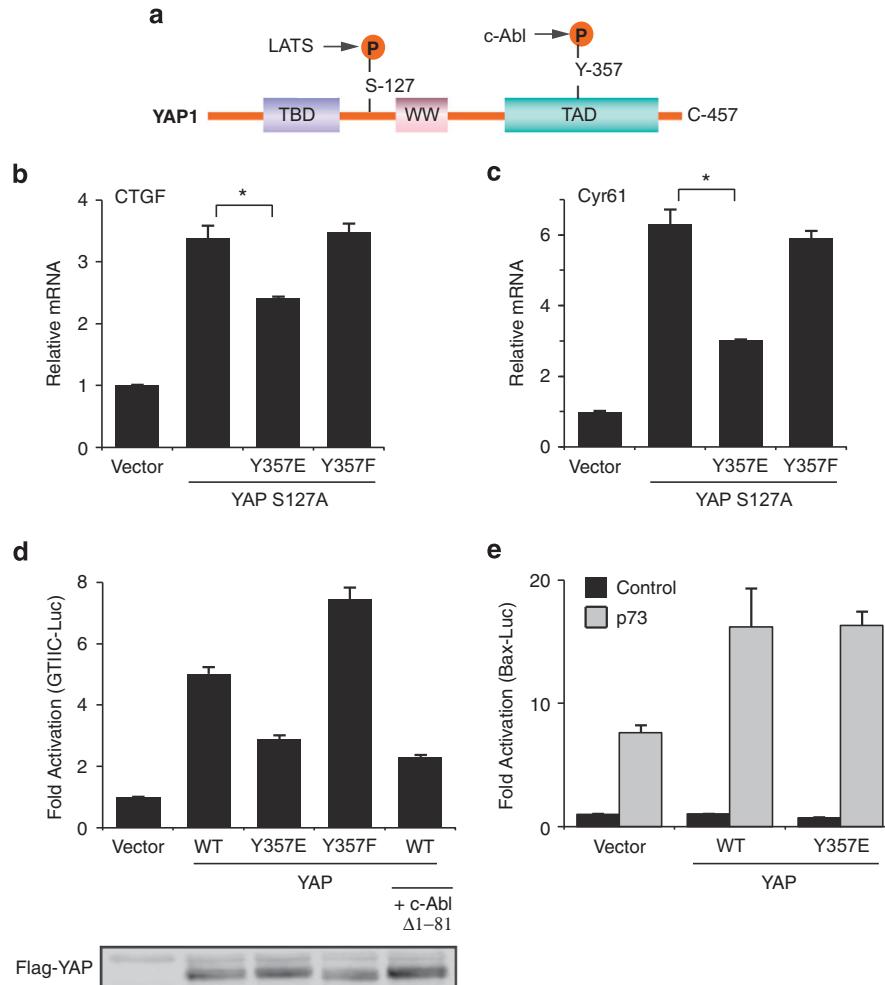


**Figure 4** The phosphomimetic Y357E mutation is inefficient in induction of TEAD targets by YAP. **(a)** Structural features and main phosphorylation sites of YAP1. Illustrated here are three major motifs: a TEF/TEAD-binding (TBD) domain, a WW domain, and a transcriptional activation (TAD) domain. The letter 'P' denotes phosphorylation, either on serine 127 by LATS or on tyrosine 357 by c-Abl. **(b and c)** Y357E mutation reduces expression of TEAD-driven genes. MCF10A cells were infected with either empty vector (pBabe puro) or the indicated plasmids. Gene expression level was determined by quantitative RT-PCR and compared with vector control cells (\* $P < 0.05$ ). **(d)** Y357E mutation inhibits YAP coactivation of TEAD on a TEAD-responsive element. The designated plasmids were co-transfected with a TEAD-responsive element luciferase reporter plasmid (8xGT11C-Luc) into HEK293 cells. Luciferase activity was measured and normalized to co-transfected TK-*Renilla*. Flag-YAP western blot shows that YAP expression level was not decreased by c-Abl or the Y357E mutation. **(e)** Y357E does not compromise coactivation of YAP on p73. Wild-type YAP or YAP Y357E were co-transfected with a Bax promoter luciferase reporter plasmid with or without p73 and analyzed as in **(e)**

Y357F-expressing cells showed an increased E-cadherin loss relative to the wild-type YAP-expressing cells. EMT was also evaluated by protein expression level of E-cadherin (Supplementary Figure 5a). Unlike wild-type YAP, YAP Y357E was less effective in E-cadherin suppression, indicating a reduced EMT induction. No significant changes in E-cadherin mRNA levels were found between cells expressing the different YAP constructs (Supplementary Figure 5b). These results suggest that YAP pY357 blunted its EMT-promoting capacity.

**YAP Y357E phosphomimetic mutant fails to induce cell motility and transformation.** Using the wound healing assay, we tested the effect of Y357E on YAP-induced cell motility. Although both wild-type YAP and YAP Y357F-overexpressing cells partially filled the gap within 24 h

(Figure 6c), YAP Y357E-infected cells were significantly less effective in filling the wound. To assess the anchorage-independent growth potential of the cells, the different established cell lines were seeded in soft agar for 21 days. Whereas control cells formed no colonies, significant colony formation was seen in both wild-type YAP and YAP Y357F-infected cells (Figure 6d). In contrast, cells overexpressing YAP Y357E showed a marked reduction in their ability to form colonies in soft agar. It is also interesting to note that both migratory potential and anchorage independence are moderately enhanced in the YAP Y357F phosphodead mutant overexpressing cells as compared with wild-type YAP, possibly because this mutant escaped the endogenous c-Abl. These data suggest that YAP Y357 phosphorylation impairs its effects on cell transformation, migration, anchorage-independent growth, and EMT.

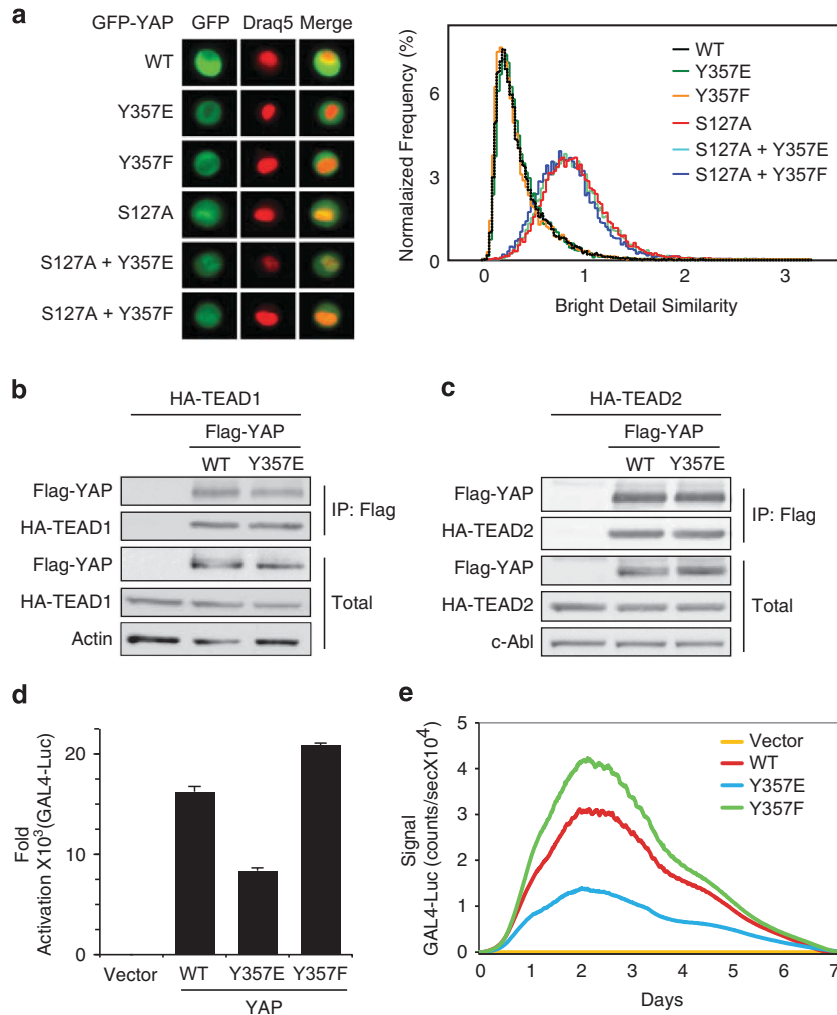


**Figure 5** Y357E mutation specifically inhibits TEAD coactivation by YAP without altering intracellular localization or TEAD binding. (a) Mutations on tyrosine 357 do not alter YAP nuclear–cytoplasmic localization. Different GFP-YAP plasmids were stably expressed in MCF10A cells by retroviral infection. MCF-10A cells stably expressing GFP-YAP were trypsinized, washed, and stained with nuclear probe DRAQ-5. Then, 20 000 cells of each type were analyzed by ImageStream-X. Left panel: fluorescent microscopic images of single cells. Right panel: colocalization of GFP-YAP and nuclear probe was estimated by using the Bright Detail Similarity R3 feature. (b and c) Y357E mutation does not alter YAP interaction with TEAD. HEK293 cells were transfected with Flag-tagged YAP constructs and either HA-tagged TEAD1 (b) or TEAD2 (c) and analyzed by co-immunoprecipitation. Actin (b) or c-Abl (c) served as protein loading controls. (d and e) Y357E mutation compromises YAP coactivation on TEAD transactivation domain. Gal4-fused TEAD was co-transfected with a Gal4-luc reporter into HEK293 cells in the presence of either wild type, Y357E YAP, or Y357F YAP. In (d), luciferase activity was measured after 72 h. Luciferase activity in the absence of YAP was set to 1. In (e), the same experiment was conducted with real-time bioluminescence recorded over time

## Discussion

In this study, we show that DNA damage and the nonreceptor tyrosine kinase c-Abl act as negative regulators of TEAD coactivation by YAP. Previously, we reported that under DNA damage c-Abl is activated and phosphorylates YAP at the Y357 residue (pY357).<sup>24</sup> YAP pY357 shows an increased association with p73 in targeting pro-apoptotic genes. Here we report that under DNA damage, the YAP–TEAD target genes are poorly expressed, that this inhibitory effect involves activation of c-Abl and that active c-Abl is sufficient in obtaining this effect. Inhibition of YAP–TEAD transcription by c-Abl is reflected physiologically by the inhibition of YAP transforming activity by c-Abl. By employing the phosphomimetic mutant approach, we were able to corroborate the role of pY357 in this process.

Not much is known about the post-translational modification of TEAD transcription factors. We found that c-Abl phosphorylates TEAD1 but not TEAD2. However, as the coactivation of both TEADs by YAP is much lower in the presence of c-Abl, we do not think that TEAD1 phosphorylation plays a major role in this process. Moreover, we have provided evidence for YAP pY357 and YAP Y357E phosphomimetic mutant to exhibit poor TEAD coactivation. The fact that lack of coactivation was also observed at the level of the GAL4–TEAD reporter assay suggests that YAP–TEAD support transcription via a specific but yet unknown transcription mediator.

YAP Y357 residue is potentially a phosphorylation target for several tyrosine kinases, including c-Abl, Yes, and Src.<sup>24,25,30</sup> Using the phosphomimetic YAP mutant allowed us to investigate how phosphorylation of this site may affect YAP activity regardless of the identity of the phosphorylating

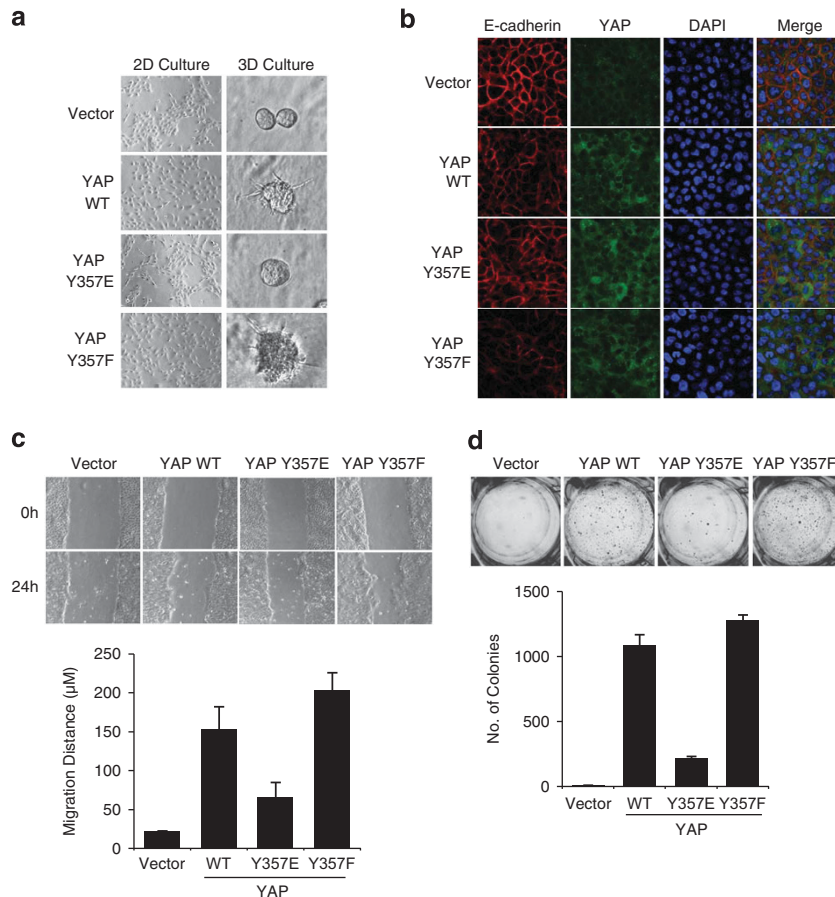


**Figure 6** Y357E mutation inhibits phenotypic effects of YAP in MCF10A cells. **(a)** Y357E mutation inhibits YAP-induced EMT. MCF10A cells were infected with either empty vector (pBabe puro), YAP wild type, YAP Y357E, or YAP Y357F. The 2D morphology – representative images of cells grown in monolayer cultures; 3D morphology – cells were cultured on Matrigel. Images were taken on day 4. **(b)** YAP Y357E is defective in reducing membrane E-cadherin. The indicated MCF10A stable cells were stained by anti-E-cadherin (red), YAP (green), and DAPI (blue). **(c)** Y357E mutation inhibits YAP-induced enhanced migration potential as measured in a wound healing assay. Confluent cells were scratched using 1 ml pipette and grown for 24 h in medium containing 2% serum and no EGF. **(d)** Y357E mutation inhibits YAP-induced anchorage independence. Images taken and colonies counted 21 days after cells were seeded in soft agar. Colonies  $> 50 \mu\text{m}$  in diameter were counted as positive for growth. Assays were conducted in three independent experiments

kinase. Interestingly, all our analyses indicated that the phosphodead Y357F mutant was even more potent than the wild type, hinting toward the possibility that this mutant escaped the negative effect of phosphorylation by the endogenous c-Abl. In any case, the YAP Y357F mutant served to rule out the possibility that effects of the Y357E mutation are the result of a direct role of the naive Y357, like maintenance of YAP configuration.

Although the Hippo pathway controls YAP through serine phosphorylation that promotes its sequestration and degradation, in this study we identified tyrosine phosphorylation as an additional means of regulation. However, unlike modification on serine residues, tyrosine phosphorylation does not result in subcellular sequestration or destabilization of YAP but rather rewires its transcriptional programs by targeting pro-apoptotic genes and generating an abortive complex with TEAD to inhibit proliferation and activation of survival genes. CTGF, the major TEAD target, functions as an anti-apoptotic mediator<sup>31</sup> and it is downregulated by active c-Abl and DNA damage. These findings are coherent with a model whereby in the

process of the DNA damage response two arms are activated; one blocks the expression of the anti-apoptotic survival genes and the other induces the expression of the proapoptotic genes (Figure 7).

Moreover, this study further corroborates the cross-talk between the Hippo pathway and DNA damage signaling. In crowded cells, where the Hippo pathway is functional, activated Lats phosphorylates c-Abl to downregulate its kinase activity,<sup>32</sup> suggesting the domination of Hippo over the DNA damage pathway. Hippo pathway cross-talks with other signaling pathways to orchestrate cell-fate decisions was lately reinforced in studies outlining the connection of Hippo components with the PI(3)K–mTOR pathway, Wnt/ $\beta$ -catenin pathway, and mechanotransduction.<sup>33–35</sup>

Our findings that active c-Abl functions as a switcher between different transcriptional programs might explain its tumor suppressor function. It was reported that c-Abl counteracts TGF- $\beta$ -mediated transformation and EMT,<sup>16</sup> but the underlying mechanism was unclear. Recently, it has been shown that an important way by which TGF- $\beta$  promotes tumor



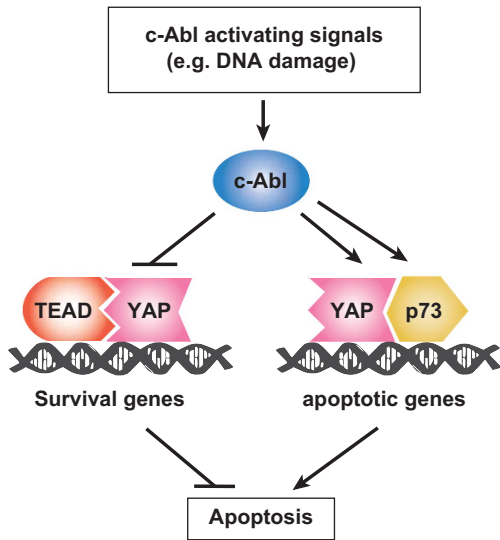


**Figure 7** YAP task assignment is regulated through phosphorylation by c-Abl: a model. When the Hippo pathway is inactive, as in proliferating cells, YAP coactivates TEAD to express survival genes involved in suppression of apoptosis. Under DNA damage, c-Abl is activated and phosphorylates p73 and YAP. These modifications lead to YAP-p73-induced transcription of pro-apoptotic genes. Simultaneously, phosphorylation of YAP by c-Abl inhibits its potential to coactivate TEAD, resulting in blunting of expression of anti-apoptotic genes and promotion of apoptosis

cell growth is through YAP and TEAD.<sup>36</sup> When tumor cells are treated with TGF- $\beta$ , SMAD3 forms a complex with YAP and TEAD on the CTGF promoter, resulting in its activation. c-Abl inhibition of TGF- $\beta$ -induced mammary cell transformation can be explained by our finding that c-Abl renders YAP incompetent in coactivating TEAD.

Phosphorylation on the YAP Y357 residue by the tyrosine kinase YES1 was recently shown to promote the transforming properties of YAP.<sup>25</sup> This is the case in a subset of colon tumor cells overexpressing  $\beta$ -catenin through a  $\beta$ -catenin-dependent pathway. It is possible that Wnt signaling via  $\beta$ -catenin keeps the tyrosine phosphorylated YAP functional as a coactivator by generating a unique complex at the target promoters. This context-dependent function of tyrosine phosphorylated YAP deserves further studies in the future.

The fact that tyrosine phosphorylation of YAP plays important roles in regulating the Hippo pathway has been recently supported by findings on YAP association with specific phosphotyrosine phosphatases: protein tyrosine phosphatase nonreceptors 14 and 11 (PTPN14 and PTPN11).<sup>37–42</sup> It was found that cytoplasmic PTPN14 inhibits oncogenic activity of YAP by binding and sequestering it from the nucleus. Interestingly, PTPN14 translocation to the nucleus is associated with induction of proliferation.<sup>43</sup> An interesting possibility is that nuclear PTPN14 supports proliferation by dephosphorylation of the phosphorylated YAP at Y357, whereas the cytoplasmic protein causes the opposite effect by regulating YAP in a phosphatase-independent manner.

Finally, in this study we described an important regulatory role for c-Abl and Y357 phosphorylation in YAP-induced transformation and EMT that places c-Abl and the DNA

damage response in general as potential key elements in regulation of the oncogenic properties of YAP. This may help in the future to develop strategies to utilize c-Abl activation to treat YAP-associated cancer. This might be achieved either physiologically by inducing DNA damage or pharmacologically by formulating c-Abl-inducer drugs.

## Materials and Methods

**Cells and cell culture.** The cell lines used were human embryonic kidney cells HEK293 and HEK293 Phoenix and the non-transformed human breast epithelial cell line MCF10A. HEK293 and human hepatocellular carcinoma HepG2 cells were grown in Dulbecco's modified Eagle's medium (DMEM; GIBCO, Grand Island, NY, USA) supplemented with 8% fetal bovine serum (GIBCO), 100 units/ml penicillin, and 100  $\mu$ g/ml streptomycin, and cultured at 37 °C in a humidified incubator with 5% CO<sub>2</sub>. Human small-cell lung carcinoma H1299 cells were grown in RPMI (GIBCO) supplemented with 8% fetal bovine serum (GIBCO), 100 units/ml penicillin, and 100  $\mu$ g/ml streptomycin. MCF10A were grown in DMEM/F12 (Biological Industries, Kibbutz Beit Haemek, Israel) supplemented with 5% donor horse serum (GIBCO), 2 mM glutamine (Biological Industries), 20 ng/ml epidermal growth factor (EGF), 10  $\mu$ g/ml insulin, 0.5  $\mu$ g/ml hydrocortisone, 100 ng/ml cholera toxin (all from Sigma-Aldrich, Rehovot, Israel), and antibiotics, as above. Light microscopy photographs of cells were performed using an IX70 microscope (Olympus, Center Valley, PA, USA) connected to a DVC camera.

**Plasmids, transfection and mRNA analysis.** pCDNA c-Abl  $\Delta$ 1-81 and pCDNA c-Abl  $\Delta$ 1-81 K290H (kinase dead) have been previously described.<sup>32</sup> pCDNA3-HA-TEAD1 was cloned from pPGS-3HA-TEAD1, kindly provided by KL Guan (Addgene, Cambridge, MA, USA; plasmid no. 33050). PCS2-HA-TEAD2 was constructed by inserting an HA tag at the N-terminus of PCS2-TEAD2 (kindly provided by H Sasaki). The GT1C reporter plasmid was a kind gift of H Sasaki. pCMX-GAL4-TEAD4 was kindly provided by KL Guan (Addgene, plasmid no. 33105). The Bax promoter luciferase construct and the GAL4 luciferase reporter have been previously described.<sup>24,44</sup> The Y357E, Y357F, and S127A mutations in pCDNA Flag YAP1<sup>24</sup> were generated by site-directed mutagenesis. pBabe retroviral vectors were previously described.<sup>45</sup> The c-Abl  $\Delta$ 1–81, Flag YAP1 wild-type, Flag YAP Y357E, and Flag YAP Y357F constructs were cloned into pBabe puro. Flag YAP1 wild type was also cloned into pBabe zeo. pBabe hygro GFP-YAP plasmids used in intracellular localization imaging were generated by cloning from Flag YAP1 wild type, Flag YAP Y357E, Flag YAP Y357F, and Flag YAP S127A. To generate cell lines stably expressing c-Abl  $\Delta$ 1–81 or the different YAP constructs, retrovirus infection was performed by transfecting 293 Phoenix retrovirus packaging cells with pBabe puro c-Abl $\Delta$ 1–81, either pBabe puro or pBabe zeo Flag YAP, or the respective empty vectors. At 48 h after transfection, viral supernatant was filtered through a 0.45- $\mu$ m filter, supplemented with 8  $\mu$ g/ml polybrene, and used to infect MCF10A cells. At 24 h after infection, cells were selected with either 2  $\mu$ g/ml Puromycin (Sigma-Aldrich) or 30  $\mu$ g/ml Zeocin (Invitrogen, Life Technologies, Carlsbad, CA, USA) in the culture medium. All transfections were done by the calcium phosphate method as previously described.<sup>26</sup> Total RNA was extracted using the Perfect Pure RNA cultured cell kit (5 PRIME, Gaithersburg, MD, USA) and then reverse transcribed by iScript cDNA synthesis kit (Bio-Rad, Hercules, CA, USA). Quantitative RT-PCR was performed with SYBR Green PCR Master Mix (Kapa Biosystems, Woburn, MA, USA) using the LightCycler 480 Instrument (Roche Diagnostics, Basel, Switzerland). Sequences of the oligos used in this study are listed in Supplementary Table 1.

**$\gamma$ -Ray irradiation.** Cells were subjected to  $\gamma$ -radiation in a Millenium 870LC Irradiator with a <sup>137</sup>Cs source (Mainance International Ltd, Waterlooville, UK).

**Immunoblot and co-immunoprecipitation studies.** Immunoblots and immunoprecipitations (IPs) were done as previously described.<sup>26</sup> The antibodies used were: anti-HA, monoclonal anti- $\beta$ -actin, anti-Flag M2, and anti-Flag M5 (Sigma-Aldrich); anti c-Abl K12 (Santa Cruz Biotechnology, Santa Cruz, CA, USA); and anti-E-cadherin (BD Biosciences, Franklin Lakes, NJ, USA). For IP of Flag-tagged proteins, anti-Flag M2 agarose beads (Sigma-Aldrich) were used. Horseradish peroxidase-conjugated secondary antibodies were from Jackson Laboratories (West Grove, PA, USA). Enhanced chemiluminescence was performed

with the EZ-ECL kit (Biological Industries) and signals were detected by the ImageQuant LAS 4000 (GE Healthcare, Piscataway, NJ, USA).

**Reporter gene assays.** HEK293 cells were transfected with indicated constructs along with a promoter-containing firefly luciferase reporter plasmid, and a *Renilla* luciferase-expressing plasmid as a transfection control. At 36 h after transfection, cell lysates were analyzed for luciferase activity in the Modulus microplate multimode reader (Turner Biosystems, Sunnyvale, CA, USA), and differences in transfection efficiency were corrected for by normalizing the firefly luciferase activity to that of *Renilla* luciferase. Real-time bioluminescence recordings were performed with a LumiCycle machine (Actimetrics, Wilmette, IL, USA).

**Imaging flow cytometry.** MCF10A cells stably expressing different GFP-YAP constructs were trypsinized, washed, and stained with nuclear probe DRAQ5 (Thermo Scientific, Waltham, MA, USA). Then, 20 000 cells of each type were analyzed by ImageStream-X (Amnis, Seattle, WA, USA), using the IDEAS software (Amnis). Colocalization of GFP-YAP and nuclear probe was estimated by using the Bright Detail Similarity R3 feature (Amnis). Median nuclear signal of the designated GFP-mutant YAP constructs was calculated as fold change from that of GFP-YAP wild type.

**Immunofluorescence analysis.** Cells were fixed with 4% paraformaldehyde for 30 min. Fixed cells were permeabilized with 0.5% Triton-X 100 and blocked with fetal calf serum containing 10% (v/v) skim milk. Cells were then incubated with mouse monoclonal anti-E-cadherin (no. 610181, BD Transduction Laboratories, BD Biosciences) or rabbit polyclonal anti Yap (H-125, Santa Cruz Biotechnology). Following incubation with Alexa Fluor 555 or 488-conjugated secondary antibodies (Invitrogen), coverslips were mounted in DAPI Fluoromount-G (SouthernBiotech, Birmingham, AL, USA). Microscopic images were obtained using laser scanning microscope LSM710 (Carl Zeiss, Microimaging GmbH, Göttingen, Germany) with plan-apochromat 63×/1.40 oil DIC M27 objective, and managed by Laser Sharp 2000 software (Zeiss, Munich, Germany). Representative images with identical laser intensities were taken from each sample.

**Soft agar assay.** Cells ( $3 \times 10^4$ ) were added to 0.5 ml of growth medium with 0.4% agar and layered onto 0.5 ml of 0.5% agar beds in 24-well plates. Cells were fed with 50  $\mu$ l of medium every 7 days for 3 weeks, after which colonies were photographed using a MZ16F binocular microscope (Leica, Wetzlar, Germany). Colonies  $>50 \mu$ m in diameter were counted as positive for growth.

**Three-dimensional morphogenesis assay.** Cells ( $1 \times 10^4$ ) were added to 0.4 ml of growth factor-reduced 2% reconstituted basement membrane (Matrigel; BD Biosciences) and layered onto 40  $\mu$ l of 100% Matrigel in Lab-TekII chamber slides (Nunc, Thermo scientific). Cells were photographed after 4 days in culture.

**Wound healing assay.** Cells were grown to confluency in six-well plates, scratched using 1 ml pipette, and grown for 24 h in medium containing 2% serum and no EGF. Cells were photographed immediately and 24 h after wound formation.

**Statistical analysis.** All values presented in graphs represent the average of at least three independent experiments if not stated otherwise. To estimate distribution of values, S.E. was calculated. The two-tailed Student's *t*-test was used to verify statistical significance.

### Conflict of Interest

The authors declare no conflict of interest.

**Acknowledgements.** We thank H Sasaki and KL Guan for the plasmid constructs and G Asher for his assistance in real-time bioluminescence recording. This work was supported by grants from the Israel Science Foundation (Grant No. 551/11) and from the Minerva Foundation with funding from the Federal German Ministry for Education and Research.

1. Harvey K, Tapon N. The Salvador-Warts-Hippo pathway - an emerging tumour-suppressor network. *Nat Rev* 2007; **7**: 182–191.
2. Pan D. Hippo signaling in organ size control. *Genes Dev* 2007; **21**: 886–897.

3. Saucedo LJ, Edgar BA. Filling out the Hippo pathway. *Nat Rev Mol Cell Biol* 2007; **8**: 613–621.
4. Camargo FD, Gokhale S, Johnnidis JB, Fu D, Bell GW, Jaenisch R et al. YAP1 increases organ size and expands undifferentiated progenitor cells. *Curr Biol* 2007; **17**: 2054–2060.
5. Dong J, Feldmann G, Huang J, Wu S, Zhang N, Comerford SA et al. Elucidation of a universal size-control mechanism in Drosophila and mammals. *Cell* 2007; **130**: 1120–1133.
6. Zhao B, Wei X, Li W, Udán RS, Yang Q, Kim J et al. Inactivation of YAP oncoprotein by the Hippo pathway is involved in cell contact inhibition and tissue growth control. *Genes Dev* 2007; **21**: 2747–2761.
7. Sudol M, Harvey KF. Modularity in the Hippo signaling pathway. *Trends Biochem Sci* 2010; **35**: 627–633.
8. Salah Z, Aqeilan RI. WW domain interactions regulate the Hippo tumor suppressor pathway. *Cell Death Dis* 2011; **2**: e172.
9. Zhao B, Li L, Tumaneng K, Wang CY, Guan KL. A coordinated phosphorylation by Lats and CK1 regulates YAP stability through SCF(beta-TRCP). *Genes Dev* 2010; **24**: 72–85.
10. Hao Y, Chun A, Cheung K, Rashidi B, Yang X. Tumor suppressor LATS1 is a negative regulator of oncogene YAP. *J Biol Chem* 2008; **283**: 5496–5509.
11. Shivelman E, Lifshitz B, Gale RP, Roe BA, Canaani E. Alternative splicing of RNAs transcribed from the human *abl* gene and from the *bcr-abl* fused gene. *Cell* 1986; **47**: 277–284.
12. Baskaran R, Wood LD, Whitaker LL, Canman CE, Morgan SE, Xu Y et al. Ataxia telangiectasia mutant protein activates c-Abl tyrosine kinase in response to ionizing radiation. *Nature* 1997; **387**: 516–519.
13. Agami R, Blandino G, Oren M, Shaul Y. Interaction of c-Abl and p73alpha and their collaboration to induce apoptosis. *Nature* 1999; **399**: 809–813.
14. Yuan ZM, Huang Y, Whang Y, Sawyers C, Weichselbaum R, Kharbanda S et al. Role for c-Abl tyrosine kinase in growth arrest response to DNA damage. *Nature* 1996; **382**: 272–274.
15. Goldberg Z, Vogt Sionov R, Berger M, Zwang Y, Perets R, Van Etten RA et al. Tyrosine phosphorylation of Mdm2 by c-Abl: implications for p53 regulation. *EMBO J* 2002; **21**: 3715–3727.
16. Allington TM, Gallier-Beckley AJ, Schiemann WP. Activated Abl kinase inhibits oncogenic transforming growth factor-beta signaling and tumorigenesis in mammary tumors. *FASEB J* 2009; **23**: 4231–4243.
17. Guo J, Kleeff J, Zhao Y, Li J, Giese T, Esposito I et al. Yes-associated protein (YAP65) in relation to Smad7 expression in human pancreatic ductal adenocarcinoma. *Int J Mol Med* 2006; **17**: 761–767.
18. Overholzer M, Zhang J, Smolen GA, Muir B, Li W, Sgroi DC et al. Transforming properties of YAP, a candidate oncogene on the chromosome 11q22 amplicon. *Proc Natl Acad Sci USA* 2006; **103**: 12405–12410.
19. Zender L, Spector MS, Xue W, Flemming P, Cordon-Cardo C, Silke J et al. Identification and validation of oncogenes in liver cancer using an integrative oncogenomic approach. *Cell* 2006; **125**: 1253–1267.
20. Kalluri R, Weinberg RA. The basics of epithelial-mesenchymal transition. *J Clin Invest* 2009; **119**: 1420–1428.
21. Zhao B, Ye X, Yu J, Li L, Li W, Li S et al. TEAD mediates YAP-dependent gene induction and growth control. *Genes Dev* 2008; **22**: 1962–1971.
22. Zhang H, Pasolli HA, Fuchs E. Yes-associated protein (YAP) transcriptional coactivator functions in balancing growth and differentiation in skin. *Proc Natl Acad Sci USA* 2011; **108**: 2270–2275.
23. Strano S, Munarriz E, Rossi M, Castagnoli L, Shaul Y, Sacchi A et al. Physical interaction with Yes-associated protein enhances p73 transcriptional activity. *J Biol Chem* 2001; **276**: 15164–15173.
24. Levy D, Adamovich Y, Reuven N, Shaul Y. Yap1 phosphorylation by c-Abl is a critical step in selective activation of proapoptotic genes in response to DNA damage. *Mol Cell* 2008; **29**: 350–361.
25. Rosenbluh J, Nijhawan D, Cox AG, Li X, Neal JT, Schafer EJ et al. beta-Catenin-driven cancers require a YAP1 transcriptional complex for survival and tumorigenesis. *Cell* 2012; **151**: 1457–1473.
26. Levy D, Adamovich Y, Reuven N, Shaul Y. The Yes-associated protein 1 stabilizes p73 by preventing Itch-mediated ubiquitination of p73. *Cell Death Differ* 2007; **14**: 743–751.
27. Davidson I, Xiao JH, Rosales R, Staub A, Chambon P. The HeLa cell protein TEF-1 binds specifically and cooperatively to two SV40 enhancer motifs of unrelated sequence. *Cell* 1988; **54**: 931–942.
28. Pluk H, Dorey K, Superti-Furga G. Autoinhibition of c-Abl. *Cell* 2002; **108**: 247–259.
29. Taagepera S, McDonald D, Loeb JE, Whitaker LL, McElroy AK, Wang JY et al. Nuclear-cytoplasmic shuttling of C-ABL tyrosine kinase. *Proc Natl Acad Sci USA* 1998; **95**: 7457–7462.
30. Zaidi SK, Sullivan AJ, Medina R, Ito Y, van Wijnen AJ, Stein JL et al. Tyrosine phosphorylation controls Runx2-mediated subnuclear targeting of YAP to repress transcription. *EMBO J* 2004; **23**: 790–799.
31. Wang MY, Chen PS, Prakash E, Hsu HC, Huang HY, Lin MT et al. Connective tissue growth factor confers drug resistance in breast cancer through concomitant up-regulation of Bcl-xL and cIAP1. *Cancer Res* 2009; **69**: 3482–3491.
32. Reuven N, Adler J, Meltser V, Shaul Y. The Hippo pathway kinase Lats2 prevents DNA damage-induced apoptosis through inhibition of the tyrosine kinase c-Abl. *Cell Death Differ* 2013; **20**: 1330–1340.

33. Dupont S, Morsut L, Aragona M, Enzo E, Giulitti S, Cordenonsi M *et al*. Role of YAP/TAZ in mechanotransduction. *Nature* 2011; **474**: 179–183.
34. Tumaneng K, Schlegelmilch K, Russell RC, Yimlamai D, Basnet H, Mahadevan N *et al*. YAP mediates crosstalk between the Hippo and PI(3)K-TOR pathways by suppressing PTEN via miR-29. *Nat Cell Biol* 2012; **14**: 1322–1329.
35. Varelas X, Miller BW, Sopko R, Song S, Gregorieff A, Fellouse FA *et al*. The Hippo pathway regulates Wnt/beta-catenin signaling. *Dev Cell* 2010; **18**: 579–591.
36. Fujii M, Nakanishi H, Toyoda T, Tanaka I, Kondo Y, Osada H *et al*. Convergent signaling in the regulation of connective tissue growth factor in malignant mesothelioma: TGFbeta signaling and defects in the Hippo signaling cascade. *Cell Cycle* 2012; **11**: 3373–3379.
37. Poernbacher I, Baumgartner R, Marada SK, Edwards K, Stocker H. Drosophila Pez acts in Hippo signaling to restrict intestinal stem cell proliferation. *Curr Biol* 2012; **22**: 389–396.
38. Wang W, Huang J, Wang X, Yuan J, Li X, Feng L *et al*. PTPN14 is required for the density-dependent control of YAP1. *Genes Dev* 2012; **26**: 1959–1971.
39. Liu X, Yang N, Figel SA, Wilson KE, Morrison CD, Gelman IH *et al*. PTPN14 interacts with and negatively regulates the oncogenic function of YAP. *Oncogene* 2013; **32**: 1266–1273.
40. Huang JM, Nagatomo I, Suzuki E, Mizuno T, Kumagai T, Berezov A *et al*. YAP modifies cancer cell sensitivity to EGFR and survivin inhibitors and is negatively regulated by the non-receptor type protein tyrosine phosphatase 14. *Oncogene* 2013; **32**: 2220–2229.
41. Michaloglou C, Lehmann W, Martin T, Delaunay C, Hueber A, Barys L *et al*. The tyrosine phosphatase PTPN14 is a negative regulator of YAP activity. *PLoS One* 2013; **8**: e61916.
42. Tsutsumi R, Masoudi M, Takahashi A, Fujii Y, Hayashi T, Kikuchi I *et al*. YAP and TAZ, Hippo signaling targets, act as a rheostat for nuclear SHP2 function. *Dev Cell* 2013; **26**: 658–665.
43. Wadham C, Gamble JR, Vadas MA, Khew-Goodall Y. Translocation of protein tyrosine phosphatase Pez/PTPD2/PTP36 to the nucleus is associated with induction of cell proliferation. *J Cell Sci* 2000; **113**(Pt 17): 3117–3123.
44. Haviv I, Shamay M, Doitsh G, Shaul Y. Hepatitis B virus pX targets TFIIB in transcription coactivation. *Mol Cell Biol* 1998; **18**: 1562–1569.
45. Morgenstern JP, Land H. Advanced mammalian gene transfer: high titre retroviral vectors with multiple drug selection markers and a complementary helper-free packaging cell line. *Nucleic Acids Res* 1990; **18**: 3587–3596.

Supplementary Information accompanies this paper on Cell Death and Differentiation website (<http://www.nature.com/cdd>)